Poor relationships between NEON Airborne Observation Platform data and field-based vegetation traits at a mesic grassland

Stephanie Pau [1,9] Jesse B. Nippert [2] Ryan Slapikas [1] Daniel Griffith [3,4] Seton Bachle [2] Brent R. Helliker [5]

Rory C. O'Connor [6] William J. Riley [7] Christopher J. Still [8] and Marissa Zaricor [2]

[1] Department of Geography, Florida State University, Tallahassee, Florida 32306 USA
[2] Division of Biology, Kansas State University, Manhattan, Kansas 66506-4901 USA
[3] US Geological Survey Western Geographic Science Center, Moffett Field, California 94035 USA
[4] NASA Ames Research Center, Moffett Field, California 94035 USA
[5] Department of Biology, University of Pennsylvania, Philadelphia, Pennsylvania 19104 USA
[6] USDA-Agricultural Research Service, Eastern Oregon Agricultural Research Center, Burns, Oregon 97720 USA
[7] Climate and Ecosystem Sciences Division, Lawrence Berkeley National Laboratory, Berkeley, California 94720 USA
[8] Forest Ecosystems and Society, Oregon State University, Corvallis, Oregon 97331 USA

Abstract. Understanding spatial and temporal variation in plant traits is needed to accurately predict how communities and ecosystems will respond to global change. The National Ecological Observatory Network's (NEON's) Airborne Observation Platform (AOP) provides hyperspectral images and associated data products at numerous field sites at 1 m spatial resolution, potentially allowing high-resolution trait mapping. We tested the accuracy of readily available data products of NEON's AOP, such as Leaf Area Index (LAI), Total Biomass, Ecosystem Structure (Canopy height model [CHM]), and Canopy Nitrogen, by comparing them to spatially extensive field measurements from a mesic tallgrass prairie. Correlations with AOP data products exhibited generally weak or no relationships with corresponding field measurements. The strongest relationships were between AOP LAI and ground-measured LAI (r = 0.32) and AOP Total Biomass and ground-measured biomass (r = 0.23). We also examined how well the full reflectance spectra (380–2,500 nm), as opposed to derived products, could predict vegetation traits using partial least-squares regression (PLSR) models. Among all the eight traits examined, only Nitrogen had a validation R^2 of more than 0.25. For all vegetation traits, validation R^2 ranged from 0.08 to 0.29 and the range of the root mean square error of prediction (RMSEP) was 14–64%. Our results suggest that currently available AOP derived data products should not be used without extensive ground-based validation. Relationships using the full reflectance spectra may be more promising, although careful consideration of field and AOP data mismatches in space and/or time, biases in field-based measurements or AOP algorithms, and model uncertainty are needed. Finally, grassland sites may be especially challenging for airborne spectroscopy because of their high species diversity within a small area, mixed functional types of plant communities, and heterogeneous mosaics of disturbance and resource availability. Remote sensing observations are one of the most promising approaches to understanding ecological patterns across space and time. But the opportunity to engage a diverse community of NEON data users will depend on establishing rigorous links with in-situ field measurements across a diversity of sites.

Key words: airborne spectroscopy; foliar traits; functional traits; hyperspectral remote sensing; Konza Prairie; tallgrass prairie.

INTRODUCTION

The response of ecological communities to present and future climate change, altered biogeochemical cycling, and the loss of biodiversity will depend strongly on species composition and their functional traits

(Suding et al. 2008). Typically, functional trait data are collected in experimental conditions (e.g., greenhouses) or field surveys on a few key focal species selected to represent an ecosystem. Quantification of spatial and temporal variation in functional traits across and within communities is lacking, mainly because field sampling to collect species' trait data in a spatially robust context is time-consuming and labor-intensive process (Schimel et al. 2013, Asner et al. 2015, Jetz et al. 2016). So, the ability to parameterize terrestrial ecosystems in Earth System Models, and therefore to predict how plant communities and ecosystems will change in the future, is limited. To address this problem, ecologists must tackle the understanding of plant trait variation and ecosystem processes across a broad range of spatial and temporal scales and environmental gradients (Levin 1992, McGill 2010, Asner et al. 2015, Jetz et al. 2016).

A common goal in environmental sciences is to improve the landscape coverage and precision of ecological pattern and ecosystem function measurements. Small-plot studies typically require large investments of time, and interpolation is required to make landscape inference. Imaging spectroscopy (i.e., "hyperspectral" images recording many narrow spectral bands) can provide spatially continuous measurements that are directly observed and not interpolated, but their fidelity to plot-scale characterizations is often ambiguous. Therefore, a question whose answer underpins the broad application of remotely sensed data is: Do similar patterns and inferences of ecosystem properties emerge between ground measurements and remotely sensed proxies across diverse landscapes?

The National Ecological Observatory Network (NEON) is a promising platform for ecologists because it provides an unparalleled range of observations across a continental extent, with 81 field sites representing 20 unique ecoclimatic regions in North America, Hawai'i, and Puerto Rico (Kampe et al. 2010). Standardized collections of numerous measurements will be made at multiple spatial scales for a 30-yr time period. As part of NEON, the Airborne Observatory Platform (AOP) collects spatially contiguous reflectance data from their imaging spectrometer and LiDAR measurements at repeat intervals (~1–3 yr) for each site at high spatial resolution (1 m). These spatially contiguous reflectance data potentially help fill a crippling "scale gap" between species' data and other environmental datasets (Jetz et al. 2012, Schimel et al. 2013). Reflectance spectra and LiDAR data can provide information on plant function, vegetation structure, and biodiversity (Ustin et al. 2004, 2009, Cavender-Bares et al. 2017). National Ecological Observatory Network also produces data products derived from the reflectance spectra and LiDAR, such as Total Biomass, Leaf Area Index (LAI), Canopy Nitrogen, and Ecosystem Structure. These derived data products are more intuitive for many ecologists compared to the full reflectance spectra. Derived products

and normalized vegetation indices can also be compared across sites, time periods, and sometimes different sensors because errors in absolute measurements are eliminated for the different site- and sensor-specific conditions.

Early research on mapping plant functional traits with airborne imaging spectroscopy focused on canopy chemistry in forest and Mediterranean ecosystems (e.g., Wessman et al. 1988, Roberts et al. 1998, Ustin et al. 1998, Ollinger and Smith 2005, Asner and Martin 2009, 2011). More recent work has demonstrated the ability to predict and map foliar traits and composition of species across several biomes enabled by NEON AOP (Chadwick et al. 2020, Chlus et al. 2020, Scholl et al. 2020, Wang et al. 2020). For example, Wang et al. (2020) mapped 26 foliar traits with AOP imaging spectroscopy data across seven NEON ecoregions with R^2 values ranged between 0.28 and 0.82. Scholl et al. (2020) used multiple AOP data products (e.g., Ecosystem Structure and Canopy Nitrogen) to classify species composition of individual tree crowns in a subalpine coniferous forest. Critically, the reliability of AOP data depends on establishing rigorous links with in-situ field measurements.

Given that NEON publishes AOP data in a publicly and freely available fashion at 1 m spatial resolution, it is imperative that researchers can understand how data were produced, and trust that they can use them without the requirement of validating data products. Here, we examine the relationships between spatially extensive plot-level trait measurements and AOP data in a wellstudied North American tallgrass prairie, Konza Prairie. First, we examine the relationships between groundbased measurements and readily available derived products of NEON AOP, such as Total Biomass, LAI, Canopy Nitrogen, and Ecosystem Structure (Canopy Height Model [CHM]), Second, we compare ground measurements with the full AOP reflectance spectra.

METHODS

Study site

Konza Prairie Biological Station, part of NEON Domain 06 (KONZ), is a 3,784 ha tallgrass prairie in northeastern Kansas, USA (39°05 N, 96°35 W). The average annual

precipitation is 835 mm and the average annual air temperature is 13°C. Aboveground tree biomass, productivity, and vegetation structure are dominated by a few perennial C_4 species. There is a highly diverse community of C_3 grass, forb, and woody species (>600 species) that co-occur within this grassland, but at low abundances relative to C_4 grasses (Freeman and Hurlbert 1985, Towne 2002). Variation in vegetation traits changes due to the experimental template of fire and grazing that exists at Konza Prairie (Fig. 1). Within scales <2,500 m^2, vegetation traits are often dominated by C_4 grasses in areas with frequent burning (<4 yr; Nippert et al. 2011). At our scale of inquiry, vegetation traits measured in 1-m^2 plots should be similar to the surrounding pixels.

Field measurements and sample processing

During 8 and 14 June 2017, we sampled 200 1-m^2 plots, randomly located across Konza Prairie using ArcGIS 10.1. Plots were selected to span the breadth of topographic gradients and long-term fire × grazing contrasts that exist within this location. In the field, some locations were slightly shifted to avoid heavily wooded or riparian areas, as well as roads, which delineate different treatments. Leaf Area Index was measured using a LAI-2000 Plant Canopy Analyzer (Li-COR, Lincoln,

m^2 square clip frames, with one replicate per plot. Biomass was sorted into grass (live and dead litter), forb, and woody vegetation. Total biomass was calculated as the sum of grass, forb, and woody biomass (not including litter).

Biomass samples were dried in an oven at 60°C for 72 h before weighing to the nearest 0.01 g. Before chemical analysis, dried plant tissue was ground using a Wiley mill and Wig-L-Bug ball mill grinder. Samples of homogenized ground tissue from each of the field plots were measured for stable Carbon and Nitrogen isotope ratios and elemental concentrations. Samples were combusted with a CE1110 elemental analyzer (Carlo Erba Instruments, Milan, Italy) and coupled to a Delta Plus mass spectrometer (Thermo Electron Corporation, Bremen, Germany) for isotope analysis using a ConFlo II Universal Interface (Thermo Electron Corporation, Bremen, Germany) in the Stable Isotope Mass Spectrometry Laboratory (SIMSL) at Kansas State University. The isotopic ratio of samples was calculated using delta notation as: $\delta = [(R_{sample}/R_{standard} - 1) \times 1{,}000]$, where R is the ratio of the heavy to light isotopes for the sample and standard, respectively. The within-run variability for $\delta^{13}C$ (isotopic composition of carbon) estimated as the SD of working standards, varied between 0.03 and 0.06‰ across runs. The within-run variability for $\delta^{15}N$
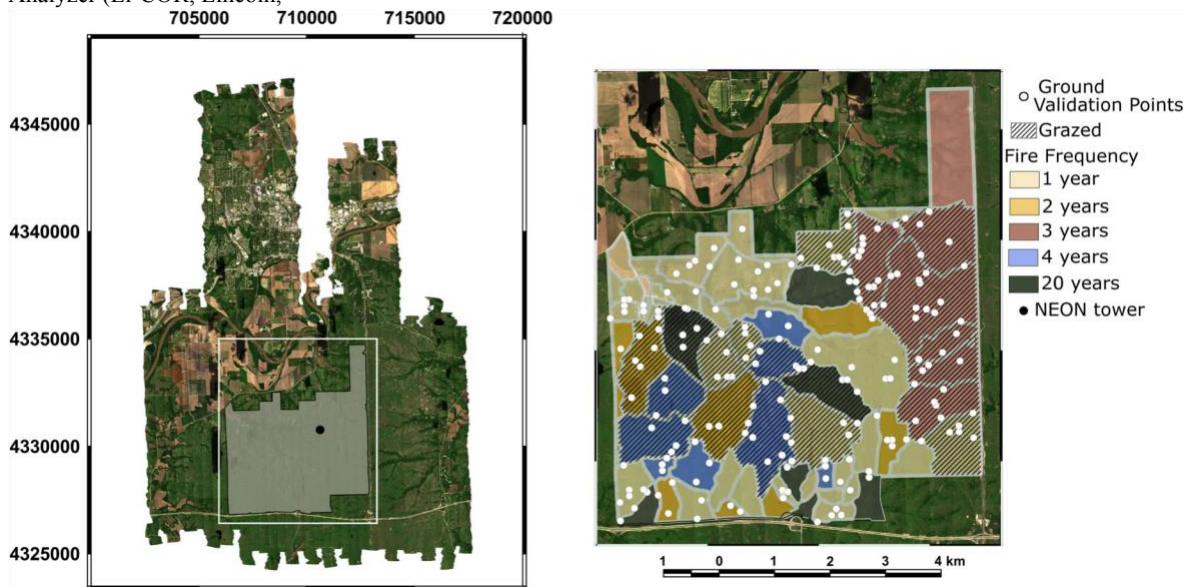

FIG. 1.   NEON AOP flightlines with Konza Prairie in white box (left); and locations of 200 ground validation field plots, which capture high variability in grazing and fire regimes (right).

(isotopic composition of nitrogen) varied between 0.07 and 0.11‰ across runs.

NE) within the center of each plot. Maximum canopy height was measured for both the tallest herbaceous and woody (when present) species within each plot. Plant species identity was recorded for all species >10% cover within each plot. Aboveground biomass was harvested within 0.1-

AOP data

We downloaded NEON's LiDAR-derived Ecosystem Structure CHM (DP3.30015.001; accessed 1 June 2020), reflectance-derived Canopy Nitrogen (DP3.30018.001; accessed 1 June 2020), LAI (DP3.30012.001; accessed 1 June 2020), Total Biomass (DP3.30016.001; accessed 1 June

2020), and the full orthorectified surface reflectance data (DP3.30006.001; accessed 1 June 2020) for NEON′s 2017 KONZ site collections. The Ecosystem Structure CHM is derived from LiDAR point cloud data. A continuous surface representing the height at the top of the canopy (m) is produced. The Canopy Nitrogen product is based on the Normalized Difference Nitrogen Index (NDNI) using reflectance at 1,510 nm (associated with the Nitrogen content of leaves) and 1,680 nm (associated with foliar biomass) to estimate the relative amount of Nitrogen in vegetation (unitless). The LAI product represents the ratio of the surface area of upper leaf to ground surface area of broadleaf canopies, and is produced using an algorithm with the Soil Adjusted Vegetation Index (SAVI) as an input (unitless). The Total Biomass product (g m^{-2}) is calculated from a functional relationship using cumulative growing season NDVI from several temperate and boreal forest sites, as well as latitude for each site. For full details on each product, see NEON documentation associated with each product (https://data.neonscience.org).

Airborne Observation Platform data were extracted for the corresponding 1 m pixel over each of the 200 field plots using coordinate locations recorded in the field with a Trimble GEO5s and a Trimble GEO7, both with an accuracy of <1 m. As the vegetation traits we examined are similar within ~2,500 m^{-2} (Nippert et al. 2011), small shifts in pixel alignment due to georectification and mosaicing should not substantially affect relationships between AOP vegetation products and trait measurements from the field. Nonetheless, we additionally present results using a circular 10-m buffer around the location of each plot to average AOP data (groundbased plot data were not averaged across the buffer). Moreover, we filtered for pixels with near-infrared (NIR) reflectance ≥20% and Normalized Difference Vegetation Index (NDVI) ≥0.5 to remove possible shadows or other contaminants to well-lit vegetation pixels (Baldeck and Asner 2013).

The NEON AOP includes an imaging spectrometer covering 380–2,500 nm in 426 bands and provides a reflectance product with a spectral sampling of ~5 nm and a 1 m spatial resolution (Kampe et al. 2010). In 2017, NEON AOP flew a defined flight box over KONZ on 5 and 9 June. Flight timing was designed to capture the peak greenness of the site, determined from a 15-yr analysis of MODIS NDVI (Moderate Resolution Imaging Spectroradiometer NDVI) measurements. Images of surface reflectance were generated by NEON after processing the raw spectrometer measurements to a calibrated at-sensor radiance by applying a rigorous orthorectification and atmospheric correction. The atsensor radiance and orthorectification are determined using in-house NEON algorithms, while the atmospheric correction is determined with ATCOR-4 (ReSe Applications LLC, Wil, Switzerland; see details in data.neonscience.org/api/v0/documents/NEON.DOC.001288vA).

Analysis

We first examined Pearson correlations between AOP products and ground-based measurements. Then, we performed PLSR using the full canopy spectra to assess the ability of AOP spectral reflectance to predict ground-based field measurements. Partial least-squares regression is commonly used to evaluate relationships between spectroscopic data and functional traits (e.g., Ollinger and Smith 2005, Dahlin et al. 2013, Serbin et al. 2014). Partial least-squares regression reduces the large predictor matrix (i.e., 426 bands of reflectance) to fewer, uncorrelated latent components. Atmospheric water absorption regions (1,130–1,445 nm and 1,790– 1,955 nm) were removed due to low signal-to-noise ratio in these regions. We used the "plantspec" package (Griffith and Anderson 2019) in the R computing environment (RCore Team 2020). This package is a wrapper for the "pls"package (Wehrens and Mevik 2007) for optimizing and fitting PLSR models. The "SPXY" method, a modified Kennard-Stone algorithm implemented in "plantspec", was used to optimally split the data into representative subsets. This method considers variation in both the spectra and response values when subdividing the data and has been shown to out-perform other methods (Saptoro et al. 2012, Griffith and Anderson 2019). Seventy-five percent of the data was used for calibration and 25% of the data was used for validation. We used "plantspec" to select an optimal model with the lowest RMSEP after comparing the raw spectra to three data transformations (Constant Offset Elimination, Vector Normalization, and a Min/Max Normalization). The number of latent vectors used in the optimal model was chosen as the minimum number of factors that resulted in a predicted residual error sum of squares (PRESS) from leave-one-out cross-validation, with a probability less than or equal to 0.75. We report results from the optimal model with the lowest RMSEP.

RESULTS AND DISCUSSION

Correlations (Pearson′s r) showed generally weak or no relationships between AOP products and corresponding ground-based measurements (Table 1). Using the 10m buffer and the NIR/NDVI filter for AOP data resulted in slightly better relationships than the 1 m data and/or no filter (Table 1 and Appendix S1: Table S2). The AOP Canopy Nitrogen and CHM showed no relationships with ground-based Nitrogen or canopy height, respectively (i.e., r-value close to 0). The AOP Total Biomass and LAI products were better correlated with associated ground-based measures. Airborne Observation Platform Total Biomass, using both the 1 m pixel and the 10-m buffer, was significantly correlated with groundbased total biomass (r = 0.21 and 0.23, respectively) and grass biomass (r = 0.17 and 0.23, respectively). Airborne Observation Platform LAI, using only the 10-m buffer, was significantly correlated with ground-based LAI (r = 0.32). Although,

TABLE 1. Pearson correlation matrix of NEON AOP data products using an NIR/NDVI filter and ground-based measurements from 200 plots at Konza Prairie.

	AOP Total Biomass	AOP Total Biomass 10 m	AOP CHM	AOP CHM 10 m	AOP LAI	AOP LAI 10 m	AOP Nitrogen	AOP Nitrogen 10 m	LAI	Canopy height	Total biomass	Grass biomass	Forb biomass	C	N	$\delta_{15}N$
AOP Total Biomass 10 m	0.82***															
AOP CHM	0.24***	0.28***														
AOP CHM 10 m	0.26***	0.35***	0.92***													
AOP LAI	0.83***	0.67***	0.16*	0.14												
AOP LAI 10 m	0.72***	0.88***	0.31***	0.30***	0.72***											
AOP Nitrogen	0.73***	0.64***	0.06	0.05	0.74***	0.63***										
AOP Nitrogen 10 m	0.56***	0.73***	0.08	0.02	0.54***	0.77***	0.83***									
LAI	0.19**	0.29***	−0.10	−0.09	0.12	0.32***	0.36***	0.45***								
Canopy height	0.14	0.19**	0.09	0.11	0.04	0.13	0.18*	0.20**	0.49***							
Total biomass	0.21***	0.23***	−0.08	−0.09	0.16*	0.24***	0.22**	0.26***	0.35	0.21**						
Grass biomass	0.17*	0.23***	−0.05	−0.03	0.09	0.21***	0.29***	0.32***	0.38	0.27***	0.80***					
Forb biomass	0.11	0.08	−0.04	−0.10	0.16*	0.12	−0.03	0.01	0.07	−0.02	0.49***	−0.09				
C	−0.05	−0.06	−0.06	−0.05	−0.05	0.00	−0.05	−0.01	0.10	−0.08	0.06	0.01	0.06			
N	0.10	0.07	−0.06	−0.09	0.20**	0.10	−0.06	−0.10	−0.06	−0.12	−0.02	−0.27	0.29***	0.42***		
$\delta_{15}N$	0.19**	0.19**	0.02	0.01	0.15**	0.12	0.05	0.04	0.00	0.06	0.01	−0.08	0.11	0.07	0.41***	
$\delta_{13}C$	−0.09	0.03	−0.03	0.01	−0.13	0.00	0.08	0.20**	0.21	0.16*	0.01	0.33	−0.42***	−0.08	−0.35***	−0.18**

Notes: CHM = Ecosystem Structure Canopy Height Model; LAI = leaf area index; NDNI = Normalized Difference Nitrogen Index. Total biomass is the sum of grass, forb, and woody biomass. $P \leq 0.001$ (***), $P \leq 0.01$ (**), and $P \leq 0.05$ (*). See Appendix S1: Table S2 for results without an NIR/NDVI filter for AOP data.

AOP Total Biomass and AOP LAI showed significant correlations with ground-based measures, most of the variation in vegetation traits was not captured by the corresponding AOP product, and there are large mismatches in absolute values.

The AOP Biomass product reached a ceiling and never exceeded 40 g m^2, underestimating ground-based biomass sometimes by more than a factor of 10 (Fig. 2a). The AOP Biomass product's reliance on the NDVI may be one reason that biomass values appear to reach a low upper limit as NDVI at our plots shows the same pattern (Appendix S1: Fig. S1). Normalized Difference Vegetation Index does not continue to increase with high biomass measured in the field, possibly because of NDVI saturation. Normalized Difference Vegetation Index is known to saturate in areas of high biomass and thus is thought to be a poor index of vegetation structure and function in dense forests, but reliable in grasslands and other less structurally complex habitats (Sellers 1985, Gao et al. 2000, Goodin and Henebry 1997). The AOP Biomass product uses an algorithm developed for woody biomass in forest ecosystems. Even for forests, it is known to saturate at biomass levels greater than 180 g/ m^2 at high latitudes and greater than 60 g/m^2 at low latitudes (NEON.DOC.004363vA; Dong et al. 2003). At our tallgrass prairie site, biomass greatly exceeded 60 g/m^2
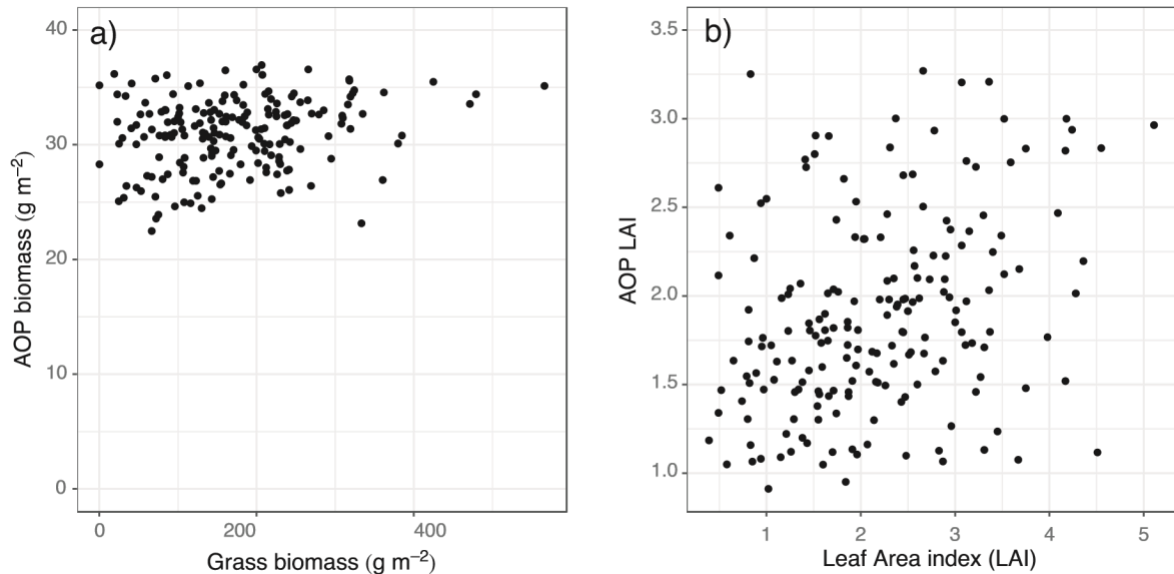
F$_{IG}$. 2. Scatterplots of NEON AOP's Total biomass (a; slope = 0.01 and intercept = 29.5) and LAI (b; slope = 0.17 and intercept = 1.52) products using an NIR/NDVI filter and a 10-m circular buffer with corresponding field measurements from 200 plots

with grass biomass averaging 170.9 g/m^2 within the first month of the 2017′s growing season. At least 5 core and 2 relocatable NEONsites are predominately grassy (Colorado Plains Experimental Range, Konza Prairie, Jornada Experimental Range, Lyndon B. Johnson National Grassland, Woodworth, Northern Great Plains Research Laboratory, and Marvin Klemme Range Research Station), and many more sites have at least some grass or herbaceous cover, where AOP products could be explored further. Our results demonstrate that there is no 1:1 relationship between AOP products and corresponding ground-based measures; however, transforming variables may improve relationships.

The AOP LAI product is also based on a spectral index, the SAVI, but it did not show a saturating relationship with our ground measurements (Fig. 2b). Leaf Area Index products developed from optical remote sensing (vs. radar or LiDAR) often saturate in dense forest canopies because the signal is predominantly driven by the top of the canopy. Instead, there is substantial scatter around a positive linear correlation at our site, where LAI is <6. Therefore, on average, increases in LAI is captured by the AOP product. However, at any specific location at the 1 m scale provided, LAI predicted from AOP observations may be highly inaccurate.

Airborne Observation Platform products were correlated with non-corresponding ground-based measures (Table 1). For example, AOP Total Biomass using the 1 m pixel and 10-m buffer, was significantly correlated with LAI (r = 0.19 and 0.29, respectively), canopy height (r = 0.16 and 0.19, respectively), and δ^{15}N (r = 0.19 and 0.19, respectively). Airborne Observation Platform LAI using the 10 m buffer was significantly correlated with total biomass (r = 0.24) and grass biomass (r = 0.21). Airborne Observation Platform

Canopy Nitrogen, using both the 1 m pixel and 10-m buffer, was significantly correlated with ground-based LAI (r = 0.36 and 0.45, respectively), canopy height (r = 0.18 and 0.20, respectively), total biomass (r = 0.22 and 0.26, respectively), and grass biomass (r = 0.29 and 0.32, respectively). These relationships suggest that spectrally derived AOP products, such as Canopy Nitrogen, are

at Konza Prairie.

largely driven by plant biomass (Homolova et al. 2013, Knyazikhin et al. 2013).

Examining the full reflectance spectra in PLS regressions, as opposed to correlations with the AOP products, revealed more promising relationships for some traits. In general, using a 10-m buffer and no NIR/NDVI filter resulted in better or similar relationships for most traits; therefore, we focus on those results (Table 2). Regardless of the spatial extent or use of a filter, R^2 never exceeded 0.30 for any trait (see Appendix S1: Table S3 for full comparison). The PLS regression models for all but one of the eight traits we examined explained less than 25% of the measured variation in each trait (Table 2; Fig. 3). The model for Nitrogen performed moderately well, at least relative to other traits (R^2 = 0.29; Fig. 3f), but worse than typically found using remote sensing to estimate plant Nitrogen (Mutanga et al. 2004, Skidmore et al. 2010, Homolova et al. 2013, Van Cleemput et al.′ 2018). Konza contains a complex mosaic of different grazing and fire regimes, which is known to affect species composition, plant productivity, and vegetation traits across the larger landscape (Fig. 1; Briggs and Nellis 1991). Thus, spatial and temporal variability in Nitrogen has been previously mapped at this site with reasonable success using airborne hyperspectral imagery (Goodin et al. 2004, Ling et al. 2014,

2019). In our model, predictions for Nitrogen were biased low at the high end of measured values (Fig. 3), either because of a saturating relationship with reflectance data and/or heteroscedasticity in measured values (i.e., an unequal range of values at the high vs. low end of these traits). For LAI, using the full spectra resulted in a lower R^2 when predicting ground-measured LAI than compared to the correlation with the AOP LAI product. This suggests that an index-based measure (i.e., a ratio of two or more regions of the reflectance curve such as the SAVI), which can normalize soil background or atmospheric effects (Huete 1988), may be more robust as a proxy for LAI at least as a relative measure. Our low predictive accuracy for LAI, another trait that tends to be well predicted in grasslands using imaging spectroscopy (Van Cleemput et al. 2018), may be because of the high LAI at this mesic tallgrass prairie site. Predictions of Carbon and $\delta^{13}C$ were particularly poor, essentially capturing none of the variations in ground-based measures.

While other studies have reported more reliable predictions of morphological and biochemical foliar traits using AOP data in PLSR models (e.g., Wang et al. 2020, Kamoske et al. 2021), we focused on a different suite of traits that correspond directly to NEON's products. Additionally, other NEON studies have leveraged greater variability in trait values across sites and biomes. For example, in Wang et al. (2020), the range of Carbon and Nitrogen values across sites was about 6 and 20 times larger, respectively, than our measurements at Konza. By design, NEON provides data across a network of sites and ecoregions allowing comparative macrosystems research; however, site comparisons are not the only purpose of NEON data. The 1 m spatial resolution AOP data should also enable high-resolution mapping for site-specific research. Yet, inaccuracies in the field and spectral data alignment in space and/or time, biases in trait measurements or AOP algorithms, and model uncertainty can lead to erroneous mapping of spatial patterns across a site.

TABLE 2. Coefficient of determination (R^2) and Root Mean Square Error of Prediction (RMSEP; in units of measurement and as % of mean value) from partial least-squares regressions (PLSR) between the AOP reflectance spectra with no NIR/NDVI filter and ground-measured traits from 200 plots at Konza Prairie.

	1 m		10 m buffer	
	Validation R^2	RMSEP (%)	Validation R^2	RMSEP (%)
LAI	0.09	1.13 (51.87%)	0.19	1.04 (47.45%)
Total biomass (g m^2)	0.13	125.83 (56.33%)	0.11	121.75 (58.45%)
Grass biomass (g m^2)	0.00	109.57 (63.88%)	0.12	107.48 (62.69%)
Canopy height (cm)	0.03	15.32 (34.23%)	0.14	13.42 (30.00%)
C (mg/g)	−0.01	6.06 (13.87%)	0.02	5.75 (13.18%)
N (mg/g)	0.13	0.36 (31.54%)	0.29	0.34 (29.54%)
δ^{13}C (‰)	0.10	4.50 (23.57%)	0.08	5.16 (27.03%)
δ^{15}N (‰)	0.14	1.39 (52.31%)	0.16	1.54 (58.14%)

Notes: See Appendix S1: Table S3 for PLSR results using NIR/NDVI filter. The value of R^2 is never greater than 0.30 in models with or without the NIR/NDVI filter at 1 m or 10 m.
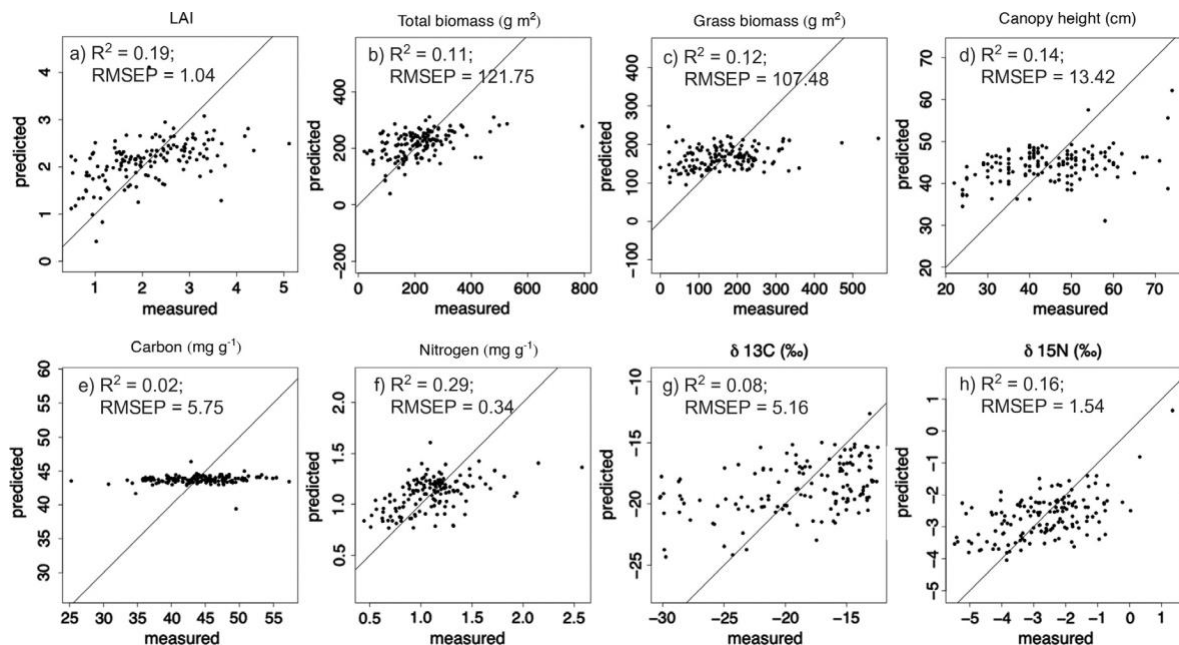

FIG. 3. Predicted vs. measured trait values from PLSR using AOP reflectance data with no NIR/NDVI filter and a 10-m circular buffer. Solid line = 1:1 relationship. Validation of R^2 is shown.

One reason for poor relationships between spectra and ground-based measurements is that mosaicked NEON products combine different flightlines with variable flight conditions (e.g., brightness) (Chadwick et al. 2020). Second, other studies that find better statistical relationships with plant traits have performed additional corrections of the reflectance data. Custom shade masks, atmospheric correction and smoothing that accounts for local topography and view-angle geometry, and access to preliminary data provided by the AOP team to collect field measurements in ideal locations could help improve relationships with ground-based data (Chadwick et al. 2020).

Our results show that ground-validation is necessary before using AOP data. Importantly, field data must also be collected appropriately to align with airborne observations (Chadwick et al. 2020, Schweiger 2020). In general, field sampling should aim for representing spatial coverage as well as sampling across trait space, which are not mutually inclusive. While we prioritized extensive sampling across geographic space, we did not always sample the full range of trait variability. For some traits such as leaf Nitrogen, greater sampling in regions with higher leaf Nitrogen levels may have improved statistical relationships. Sampling the full range of values for some traits such as leaf biochemical

traits, which may not be easy to estimate in the field, may require prior understanding of environmental features that contribute to trait changes (Schweiger 2020); although these relationships are often why trait mapping is desirable in the first place. Moreover, given the high spatial accuracy that is required for 1 m resolution airborne spectroscopy data, ground-based sampling should include a buffer (e.g., 3 × 3 pixels), within which the trait of interest is representative because of the inevitable pixels shifts in mosaicking and georectification, in addition to sensor "blurring" when radiance from neighboring pixels contribute to the signal of the focal pixel. Inamdar et al. (2020) found that only 55.5% of the signal in a pixel originated from the materials within the boundaries of that pixel. Because of the differences in the spatial scale of species turnover and variation in plant functional types at different sites, future work could assess multiple spatial extents of both field data and AOP data to find the most robust relationships.

CONCLUSION

Remote sensing observations, NEON's AOP in particular, provide unparalleled spatially contiguous, high spatial resolution, and directly observed measurements to assess vegetation structure and function. Complete spatial sampling provided by remote sensing observations is one of the most promising approaches to understanding ecological processes across scales, rather than relying on spatial averaging (Goodin and Henebry 2002, Denny 2017). The promise of mapping functional traits is persuasive because it enables ecologists to quantify how communities change over space and time in response to global change. However, the usefulness of remote sensing observations depends on establishing rigorous empirical relationships with field measurements. Sitespecific ground validation, in a diversity of sites and ecoregions, can help refine algorithms used to generate remote sensing products. In general, we found better agreement between field-measured vegetation traits and AOP data when we used a 10-m circular buffer. However, many users of NEON data may assume that the readily available 1 m data is reliable. Our analysis suggests—at least for one well-studied grassland that hosts a core NEON site—that currently available "off-theshelf" AOP data products are inaccurate and not appropriate for high-resolution mapping of vegetation traits without ground-based validation. For many of the traits measured here, no relationship exists between field measurements at the 1 m scale and AOP data. Grassy systems (grasslands and savannas) are understudied compared to trees and forests (Veldman et al. 2015, Murphy et al. 2016, Nerlekar and Veldman 2020), and grassy sites may be unexpectedly challenging for airborne spectroscopy (Van Cleemput et al. 2018). Many remote sensing scientists and ecologists typically assume grasslands to be structurally simple compared to forests. However, high species diversity within a small area (e.g., a 1 m^2 pixel), mixed functional types

of plant communities, and mosaics of disturbance and resource availability complicate remotely sensed predictions for these ecosystems. Collecting corresponding field spectra in these diverse systems (leaf- and plot-level spectra) may be critical to connecting airborne spectral observations with plot-level trait measurements from the field.

LITERATURE CITED

Asner, G. P., and R. E. Martin. 2009. Airborne spectranomics: Mapping canopy chemical and taxonomic diversity in tropical forests. Frontiers in Ecology and the Environment 7:269– 276.

Asner, G. P., and R. E. Martin. 2011. Canopy phylogenetic, chemical and spectral assembly in a lowland Amazonian forest. New Phytologist 189:999–1012.

Asner, G. P., R. E. Martin, C. B. Anderson, and D. E. Knapp. 2015. Quantifying forest canopy traits: Imaging spectroscopy versus field survey. Remote Sensing of Environment 158:15–27.

Baldeck, C. A., and G. P. Asner. 2013. Estimating vegetation beta diversity from airborne imaging spectroscopy and unsupervised clustering. Remote Sensing 5:2057–2071.

Briggs, J. M., and M. D. Nellis. 1991. Seasonal variation of heterogeneity in the tallgrass prairie: A quantitative measure using remote sensing. American Society for Photogrammetry 57:407–411.

Cavender-Bares, J., J. A. Gamon, S. E. Hobbie, M. D. Madritch, J. E. Meireles, A. K. Schweiger, and P. A. Townsend. 2017. Harnessing plant spectra to integrate the biodiversity sciences across biological and spatial scales. American Journal of Botany 104:966–969.

Chadwick, K. D., et al. 2020. Integrating airborne remote sensing and field campaigns for ecology and Earth system science. Methods in Ecology and Evolution 11:1492–1508.

Chlus, A., E. L. Kruger, and P. A. Townsend. 2020. Mapping three-dimensional variation in leaf mass per area with imaging spectroscopy and lidar in a temperate broadleaf forest. Remote Sensing of Environment 250:112043.

Dahlin, K. M., G. P. Asner, and C. B. Field. 2013. Environmental and community controls on plant canopy chemistry in a Mediterranean-type ecosystem. Proceedings of the National Academy of Sciences of the United States of America 110:6895–6900.

Denny, M. 2017. The fallacy of the average: On the ubiquity, utility and continuing novelty of Jensen's inequality. Journal of Experimental Biology 220:139–146.

Dong, J., R. K. Kaufmann, R. B. Myneni, C. J. Tucker, P. E. Kauppi, J. Liski, W. Buermann, V. Alexeyev, and M. K. Hughes. 2003. Remote sensing estimates of boreal and temperate forest woody biomass: Carbon pools, sources, and sinks. Remote Sensing of Environment 84:393–410.

Freeman, C. C., and L. C. Hurlbert. 1985. An annotated list of the vascular flora of Konza Prairie research natural area, Kansas. Transactions of the Kansas Academy of Science 88:84–115.

Gao, X., A. R. Huete, W. Ni, and T. Miura. 2000. Optical–biophysical relationships of vegetation spectrawithout background contamination. Remote Sensing of Environment 74:609–620.

Goodin, D. G., J. Gao, and J. M. S. Hutchinson. 2004. Seasonal, topographic and burn frequency effects on biophysical/ spectral reflectance relationships in tallgrass prairie. International Journal of Remote Sensing 25:5429–5445.

Goodin, D. G., and G. M. Henebry. 1997. Monitoring ecological disturbance in tallgrass prairie using seasonal NDVI trajectories and a discriminant function mixture model. Remote Sensing of Environment 61:270–278.

Goodin, D. G., and G. M. Henebry. 2002. The effect of rescaling on fine spatial resolution NDVI data: A test using multiresolution aircraft sensor data. International Journal of Remote Sensing 23:3865–3871.

Griffith, D. M., and T. M. Anderson. 2019. The 'plantspec' R package: A tool for spectral analysis of plant stoichiometry. Methods in Ecology and Evolution 10:673–679.

Homolova, L., Z. Malenovsk´ y, J. G. P. W. Clevers, G. Garcıa-´ Santos, and M. E. Schaepman. 2013. Review of optical-based remote sensing for plant trait mapping. Ecological Complexity 15:1–16.

Huete, A. R. 1988. A soil-adjusted vegetation index (SAVI). Remote Sensing of Environment 25:295–309.

Inamdar, D., M. Kalacska, G. LeBlanc, and J. P. Arroyo-Mora. 2020. Characterizing and mitigating sensor generated spatial correlations in airborne hyperspectral imaging data. Remote Sensing 12:641.

Jetz, W., et al. 2016. Monitoring plant functional diversity from space. Nature Plants 2:16024.

Jetz, W., J. M. Mcpherson, and R. P. Guralnick. 2012. Integrating biodiversity distribution knowledge: Toward a global map of life. Trends in Ecology & Evolution 27:151–159.

Kamoske, A., K. M. Dahlin, S. P. Serbin, and S. C. Stark. 2021. Leaf traits and canopy structure together explain canopy functional diversity: an airborne remote sensing approach. Ecological Applications 31:1–17.

Kampe, T. U., B. R. Johnson, M. Keller, T. U. Kampe, B. R. Johnson, and M. Kuester. 2010. NEON: The first continental-scale ecological observatory with airborne remote sensing of vegetation canopy biochemistry and structure. Journal of Applied Remote Sensing 4:043510.

Knyazikhin, Y., et al. 2013. Hyperspectral remote sensing of foliar nitrogen content. Proceedings of the National Academy of Sciences of the United States of America 110: E185–E192.

Levin, S. A. 1992. The problem of pattern and scale in ecology. Ecology 73:1943–1967.

Ling, B., D. G. Goodin, R. L. Mohler, A. N. Laws, and A. Joern. 2014. Estimating canopy nitrogen content in a heterogeneous grassland with varying fire and grazing treatments: Konza Prairie, Kansas, USA. Remote Sensing 6:4430–4453.

Ling, B., E. J. Raynor, D. G. Goodin, and A. Joern. 2019. Effects of fire and large herbivores on canopy nitrogen in a tallgrass prairie. Remote Sensing 11:1364.

McGill, B. J. 2010. Matters of scale. Science 328:575–577.

Mutanga, O., A. K. Skidmore, and H. H. T. Prins. 2004. Predicting in situ pasture quality in the Kruger National Park, South Africa, using continuum-removed absorption features. Remote Sensing of Environment 89:393–408.

Murphy, B. P., A. N. Andersen, and C. L. Parr. 2016. The underestimated biodiversity of tropical grassy biomes. Philosophical Transactions of the Royal Society B 371:20150319. https://doi. org/10.1098/rstb.2015.0319

NEON (National Ecological Observatory Network). Spectrometer orthorectified surface directional reflectance - mosaic (DP3.30006.001). https://data.neonscience.org (accessed June 1, 2020).

NEON (National Ecological Observatory Network). LAI spectrometer - mosaic (DP3.30012.001). https://data. neonscience.org (accessed June 1, 2020).

NEON (National Ecological Observatory Network). Ecosystem structure (DP3.30015.001). https://data.neonscience.org (accessed June 1, 2020).

NEON (National Ecological Observatory Network). Total biomass map - spectrometer - mosaic (DP3.30016.001). https:// data.neonscience.org (accessed June 1, 2020).

NEON (National Ecological Observatory Network). Canopy nitrogen - mosaic (DP3.30018.001). https://data.neonscience. org (accessed June 1, 2020).

Nerlekar, A. N., and J. W. Veldman. 2020. High plant diversity and slow assembly of old-growth grasslands. Proceedings of the National Academy of Sciences of the United States of America 117:18550–18556.

Nippert, J. B., T. W. Ocheltree, A. M. Skibbe, L. C. Kangas, J. M. Ham, K. B. Shonkwiler, A. Nathaniel, and N. A. Brunsell. 2011. Linking plant growth responses across topographic gradients in tallgrass prairie. Oecologia 166:1131–1142.

Ollinger, S. V., and M. Smith. 2005. Net primary production and canopy nitrogen in a temperate forest landscape: An analysis using imaging spectroscopy, modeling and field data. Ecosystems 8:760–778.

Pau, S., and J. Nippert. 2021. AOP01 Correspondence between plant traits and NEON Airborne Observatory Platform (AOP) data at Konza Prairie (2017) ver 1. Environmental Data Initiative. https://doi.org/10.6073/pasta/9c565bb6263a50185e727a267db46 b14

RCore Team. 2020. R: A language and environment for statistical computing. R Foundation for Statistical Computing, Vienna, Austria. https://www.R-project.org/

Roberts, D. A., M. Gardner, R. Church, S. Ustin, G. Scheer, and R. O. Green. 1998. Mapping chaparral in the Santa Monica Mountains using multiple endmember spectral mixture models. Remote Sensing of Environment 65:267–279.

Saptoro, A., M. O. Tade, and H. Vuthaluru. 2012. A modified´ kennard- stone algorithm for optimal division of data for developing artificial neural network models. Chemical Product and Process Modeling 7. https://doi.org/10.1515/1934-2659.1645

Schimel, D. S., G. P. Asner, and P. Moorcroft. 2013. Observing changing ecological diversity in the Anthropocene. Frontiers in Ecology and the Environment 11:129–137.

Scholl, V., M. Cattau, M. Joseph, and J. Balch. 2020. Integrating National Ecological Observatory Network (NEON) airborne

remote sensing and in-situ data for optimal tree species classification. Remote Sensing 12:1–19.

Schweiger, A. K. 2020. Spectral field campaigns: planning and data collection. Pages 385–423 in J. Cavender-Bares, J. A. Gamon, and P. A. Townsend, editors. Remote sensing of plant biodiversity. Springer International Publishing, Cham, Switzerland.

Sellers, P. J. 1985. Canopy reflectance, photosynthesis and transpiration. International Journal of Geographical Information Science 6:1335–1372.

Serbin, S. P., C. C. Kingdon, and P. A. Townsend. 2014. Spectroscopic determination of leaf morphological and biochemical traits for northern temperate for northern temperate and boreal tree species. Ecological Applications 24:1651–1669.

Skidmore, A. K., J. G. Ferwerda, O. Mutanga, S. E. Van Wieren, M. Peel, R. C. Grant, H. H. T. Prins, F. Bektas, and V. Venus. 2010. Forage quality of savannas — Simultaneously mapping foliar protein and polyphenols for trees and grass using hyperspectral imagery. Remote Sensing of Environment 114:64–72.

Suding, K. N., S. Lavorel, F. III Chapin, J. H. C. Cornelissen, S. Diaz, E. Garnier, D. Goldberg, D. U. Hooper, S. T. Jackson, and M.-L. Navas. 2008. Scaling environmental change through the community-level: A trait based response-and-effect framework for plants. Global Change Biology 14:1125–1140.

Towne, E. G. 2002. Vascular plants of Konza Prairie Biological Station: An annotated checklist of species in a Kansas Tallgrass Prairie. Sida 20:269–294.

Ustin, S. L., A. A. Gitelson, S. Jacquemoud, M. Schaepman, G. P. Asner, J. A. Gamon, and P. Zarco-Tejada. 2009. Remote sensing of environment retrieval of foliar information about plant pigment systems from high resolution spectroscopy. Remote Sensing of Environment 113:S67–S77.

Ustin, S. L., D. A. Roberts, J. A. Gamon, G. P. Asner, and R. O. Green. 2004. Using imaging spectroscopy to study ecosystem processes and properties. BioScience 54:523–534.

Ustin, S. L., D. A. Roberts, J. Pinzon, S. Jacquemoud, M. Gard-´ner, G. Scheer, C. M. Castaneda, and A. Palacios-Orueta.˜ 1998. Estimating canopy water content of chaparral shrubs using optical methods. Remote Sensing of Environment 65:280–291.

Van Cleemput, E., L. Vanierschot, B. Fernandez-Castilla,´ O. Honnay, and B. Somers. 2018. The functional characterization of grass- and shrubland ecosystems using hyperspectral remote sensing trends, accuracy and moderating variables. Remote Sensing of Environment 209:747– 763.

Veldman, J. W., et al. 2015. Toward an old-growth concept for grasslands, savannas, and woodlands. Frontiers in Ecology and the Environment 13:154–162.

Wang, Z., A. Chlus, R. Geygan, Z. Ye, T. Zheng, A. Singh, J. J. Couture, J. Cavender-Bares, E. L. Kruger, and P. A. Townsend. 2020. Foliar functional traits from imaging spectroscopy across biomes in eastern North America. New

Phytologist 228:494–511.

Wehrens, R., and B. H. Mevik. 2007. The pls package: principal component and partial least squares regression in R. https://scholar.google.com/scholar?hl=en&as_sdt=0%2C48&q=The+pls+Package%3A+Principal+Component+and+Partial+Least+Squares+Regression+in+R+Bj%C3%B8rn-Helge&btnG=

Wessman, C. A., J. D. Abert, D. L. Peterson, and J. M. Melillo. 1988. Remote sensing of canopy chemistry and nitrogen cycling in temperate forest ecosystems. Nature 335:8–10.

SUPPORTING INFORMATION

Additional supporting information may be found in the online version of this article at http://onlinelibrary.wiley.com/doi/10.1002/ecy.3590/suppinfo

OPEN RESEARCH

Data (Pau and Nippert 2021) are available from the Environmental Data Initiative at: https://doi.org/10.6073/pasta/9c565bb6263a50185e727a267db46b14